J Mater Sci (2008) 43:1757–1768
DOI 10.1007/s10853-007-2405-0

Solid-particle erosion behavior of high-performance thermoplastic polymers

Suresh Arjula · A. P. Harsha · M. K. Ghosh

Received: 17 October 2007 / Accepted: 13 December 2007 / Published online: 18 January 2008

Abstract Solid-particle erosion tests were carried out to study the effect of matrix material, impact angle, and impact velocity on the erosion behavior of seven types of thermoplastic neat polymers (i.e., polyetherimide, polyetheretherketone, polyetherketone, polyphenylene sulfide, polyethersulfone, polysulfone, and ultrahigh molecular weight polyethylene). Steady-state erosion rates of these polymers have been evaluated at different impact angles (15–90°) and impact velocities (25–66 m/s). Silica sand of particle size 200 ± 50 μm was used as the erodent. These polymers have exhibited maximum erosion rate (E_{max}) at 30° impact angle indicating ductile erosion behavior. Some of these polymers have shown an incubation behavior at lower impact velocities for an impact angle of 90°. Correlations among steady-state erosion rate and mechanical properties and glass transition temperature (T_g) were established. Morphology of eroded surfaces was examined using scanning electron microscopy and possible wear mechanisms were discussed.

Abbreviations

ABS	Acrylonitryl-butyldiene styrene
PA	Polyamide
PB	Polybutadine
PC	Polycarbonate
PE	Polyethylene
PEI	Polyetherimide
PEEK	Polyetheretherketone
PEK	Polyetherketone
PES	Polyethersulfone
PMMA	Polymetyl methacrylate
PP	Polypropylene
PPS	Polyphenylene sulfide
PS	Polystyrene
PSU	Polysulfone
PTFE	Polytetrafluoroethylene
TPI	Thermoplastic polyimide
UHMWPE	Ultrahigh molecular weight polyethylene

S. Arjula · A. P. Harsha (✉) · M. K. Ghosh
Department of Mechanical Engineering, Institute of Technology, Banaras Hindu University, Varanasi 221005, India
e-mail: harshaap@gmail.com

Introduction

High-performance thermoplastic polymers are finding increased use in aircraft components and consumer products because they posses excellent mechanical and thermal properties [1]. Material characteristics exert a strong influence on wear rate and wear mechanism in erosive wear situation [2]. According to Hutchings [3], the severity of wear can be ascertained by a dimensionless wear coefficient (k) and calculated by the following equation:

$$E = \frac{k\rho v^2}{2H}, \tag{1}$$

where E is the steady-state erosion rate, ρ is the density of material being eroded, v is the impact velocity of the particles, and H is the hardness of the target surface. For the erosion of polymers, the value of k lies typically in the range of 10^{-3}–10^{-4} where as for polymer composites in the range of 10^{-1}–10^{-3} [4]. However, it depends on the properties of material and test conditions involved which could result in changes in the value of k by some orders of magnitude.

The solid-particle erosion of neat polymers including rubbers and elastomers [5–26], and composites [27–43] was extensively studied and reported in the literature. However, erosion of bulk high-performance polymers by solid particle impact has received a little attention compared to polymer composites. It has been concluded by previous investigators that polymer composite materials had poor erosion resistance than neat polymers [29, 32]. In recent years, in many engineering applications, polymer coatings are used to increase the lives of components exposed to abrasion or erosion [44]. In view of the above, the erosion studies of bulk high-performance thermoplastic polymers by solid particle impact is required than polymer composites. The main objective of the present work was to investigate the solid-particle erosion behavior of six types of high-performance thermoplastic polymers [polyetherimide (PEI), polyetheretherketone (PEEK), polyetherketone (PEK), polyphenylene sulfide (PPS), polyethersulfone (PES), and polysulfone (PSU)] with a wide range of mechanical properties. The erosion resistance of these polymers were evaluated under consistent test conditions and compared with ultrahigh molecular weight polyethylene (UHMWPE), a general wear resistant material. The objective was to explore the correlation between erosion rate and mechanical properties of neat polymers. To the best of our knowledge, comparative studies on erosive wear behavior of these specialty polymers with in a category have not yet been reported. Hence, it becomes imperative to study the erosive wear behavior of these high-performance polymeric materials under various operating conditions. This type of study will create a large database on the erosive wear properties of high-performance thermoplastic polymers.

Experimental details

Materials selected

In the present study, six different types of high-performance thermoplastic polymers, such as PEI, PEEK, PEK, PPS, PES, and PSU were selected and the wear behavior of UHMWPE was also studied for the comparison of erosion resistance. Details of the physical, mechanical, and thermal properties are listed in Table 1. Vickers microhardness (Shimadzu microhardness tester, HMV−2) tests were performed on bulk polymers and reported in Table 1.

Methodology for evaluation of erosive wear

The details of the solid-particle erosion test rig used in the present study are shown in Fig. 1. The rig consists of an air compressor, a particle feeder, and an air particle mixing and accelerating chamber. The compressed dry air is mixed with the particles, which are fed at a constant rate from a conveyor belt-type feeder in to the mixing chamber and then accelerated by passing the mixture through a tungsten carbide converging nozzle of 4-mm diameter. These accelerated particles impact the specimen, and the specimen could be held at various angles with respect to the impacting particles using an adjustable sample holder.

Table 1 Physical, thermal, and mechanical properties of selected polymers (supplier's data)

Property	PEI	PEEK	PEK	PPS	PES	PSU	UHMWPE
Density (g/cm^3), ρ	1.27	1.30	1.30	1.40	1.37	1.24	0.93
Glass transition temperature (°C), T_g	217	148	162	90	225	190	–
Tensile strength (MPa), S	105	95	110	86	90	80	48
Tensile elongation at break (%), e	60	>50	20	36	30	>50	>350
Tensile modulus (MPa), E_1	3450	3800	4000	3600	2800	2500	689
Flexural strength (MPa)	152	160	183	145	120	100	–
Flexural modulus (GPa)	3.31	3.80	5.12	4.10	2.60	2.60	–
Izod impact, notched (J/m)	32	60	55	30	50	50	1600
Hardness (HV), H	40	28	34.4	26.5	24.2	21.4	–
Fracture toughness (MPa-m$^{1/2}$), K_{IC}	3.8	6.0	5.5	3.0	2.3	–	–
Fracture energy (kJ/m^2), G_{IC}	3.5	8.0	6.4	2.1	1.6	–	–
Supplier	GE plastics, USA	Gardha polymers, India	Victrex plc., USA	Ticona, Germany	Gardha polymers, India	BASF, Germany	Khanna polyrib, India

Fig. 1 Details of erosion test rig. (1) Sand hopper. (2) Conveyor belt system for sand flow. (3) Pressure transducer. (4) Particle-air mixing chamber. (5) Nozzle. (6) X–Y and θ axes assembly. (7) Sample holder

The feed rate of the particles can be controlled by monitoring the distance between the particle feeding hopper and the belt drive carrying the particles to mixing chamber. The impact velocity of the particles can be varied by varying the pressure of the compressed air. The velocity of the eroding particles is determined using a rotating disc method [45]. Scanning electron micrograph of silica sand is shown in Fig. 2.

Square samples of size 30 mm × 30 mm × (3–4) mm were cut from the injection molded plaques for erosion tests. The conditions under which erosion tests were carried out are listed in Table 2. A standard test procedure was employed for each erosion test. The samples were cleaned[1], dried, and weighed to an accuracy of 0.1 mg using an electronic balance, eroded in the test rig for 5 min and then weighed again to determine the mass loss. The ratio of this mass loss to the mass of the eroding particles causing the loss (i.e., testing time × particle feed rate) is then computed as dimensionless erosion rate (g/g). This procedure is repeated till the erosion rate attains a constant steady-state value.

[1] PEI, PEEK, PEK, and PPS were cleaned with acetone, whereas PES, PSU, and UHMWPE were cleaned with cotton because these polymers react with acetone.

Fig. 2 Scanning electron micrograph of silica sand

Table 2 Test parameters

Erodent	Silica sand
Erodent size (µm)	200 ± 50
Erodent shape	Angular
Hardness of silica particles (HV)	1420 ± 50
Impingement angle (α, °)	15, 30, 60, 90
Impact velocity (m/s)	25, 37, 50, 66 (±4)
Erodent feed rate (g/min)	3.6 ± 0.3
Test temperature	Room temperature
Nozzle to sample distance (mm)	10

Scanning electron microscopy of eroded samples

Scanning electron microscopy (SEM) studies were carried out on eroded samples using scanning electron microscope (ZEISS EVO® 50). The samples were silver sputtered in order to reduce charging of the surface.

Results and discussion

Erosion rate as a function of mass of erodent

Figure 3a–d shows the erosion rates of all the polymers as a function of cumulative mass of erodent at different impact angles (15–90°) and for an impact velocity of 66 m/s. These plots are obtained for determining the steady-state erosion rate. It can be seen from the curves (Fig. 3) that the erosion rate either initially increases from a low value to a high

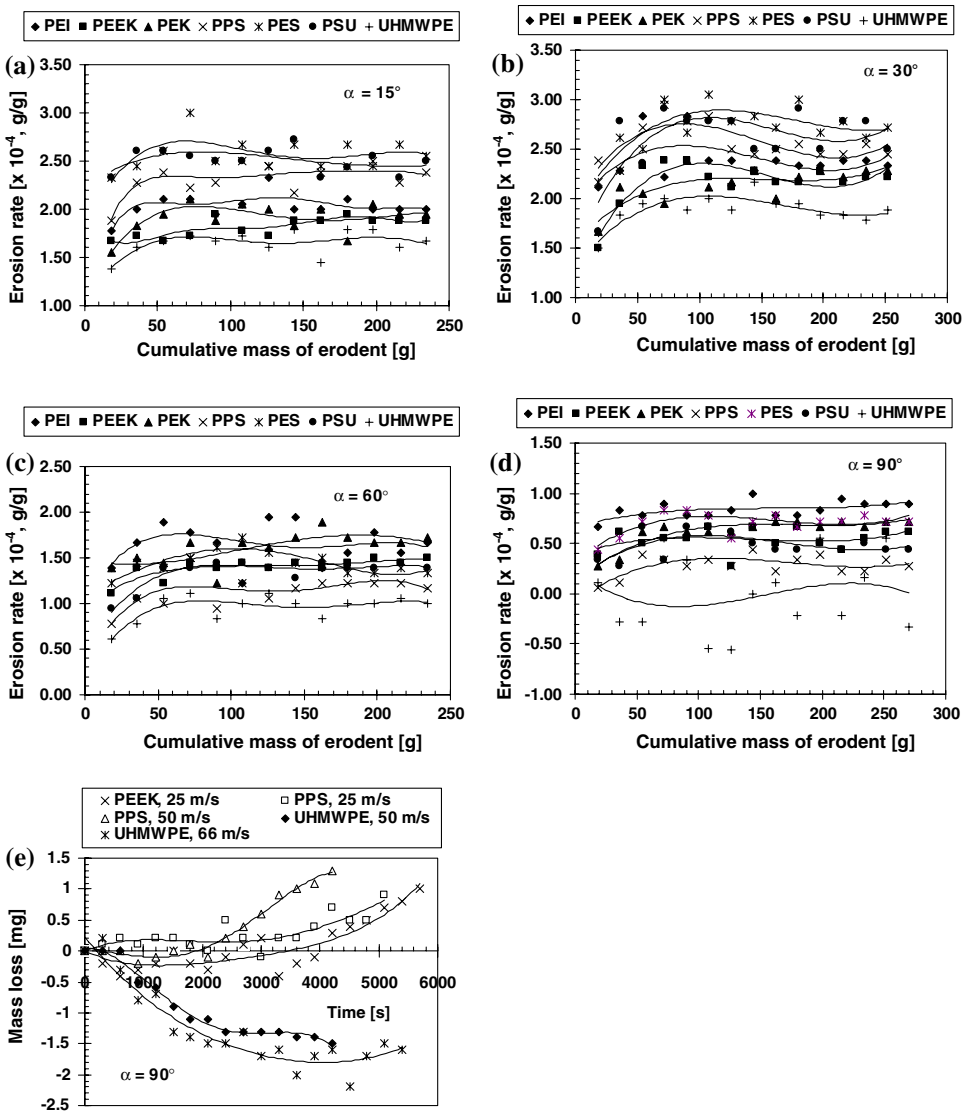

Fig. 3 Variation of erosion rate as a function of cumulative mass of erodent at different impact angles for impact velocity of 66 m/s: (**a**) 15°, (**b**) 30°, (**c**) 60°, (**d**) 90°, (**e**) typical plot of mass loss versus erosion time at 90° impact angle

value and then decreases to a constant value (i.e., acceleration, peak erosion rate, deceleration, and steady-state period) or initially increases from a low value to a constant value (i.e., acceleration and steady-state period). However, at 90° impact angle, a typical incubation period (little or no mass loss) is observed for various polymers, such as PEEK, PPS, and UHMWPE at different impact velocities (Fig. 3e). The extent of the incubation period is dependent upon the properties of polymers under the test and the impact conditions. Polymers are more susceptible to deposition of erodent during the initial stages of the test at normal impact condition [5, 27]. PEEK and PPS are semi-crystalline thermoplastics having low glass transition temperature (T_g) and hence prone to mass gain in the initial stages of erosion test. Whereas in the case of hard, amorphous, and stiffer polymers, viz. PEI, PES, and PSU, having higher glass transition temperature embedment of erodent is not observed during erosion test. It is observed from Fig. 3e that UHMWPE showed longer incubation period before a steady state is established. The incubation period with mass gain was also observed for polymers, such as polyamide (PA) [8], polypropylene (PP), polyethylene (PE), and PEEK [14]. Tilly [5] and Tilly and Sage [27] also reported the existence of incubation time in the case of polyurethane (PU) elastomers. Marie and Izvozchikov [22] proposed an erosion mechanism for elastomers involving a built-up of strain relaxation between impacts. They suggested that the strain produced by a single impact is insufficient to cause material removal and that several successive impacts are necessary to raise the strain to a sufficient level to cause material removal. This mechanism would explain the greater erosion resistance and incubation period in more resilient materials, such as elastomers and UHMWPE [18, 23, 24]. The incubation period decreases with increase in the impact velocity and decrease in the impact angle [11, 13, 15, 31]. In the literature also it was reported that for

various thermoplastic polymers (PMMA, PTFE, PC, PA, and UHMWPE) only the typical features of acceleration, peak erosion, deceleration, and stabilization are observed at oblique impact angles [8, 17, 18].

The severity of wear for various polymers is determined by the dimensionless wear coefficient (k) according to Eq. 1. Table 3 provides the values of k at different impact velocities for normal impact angle. For the erosion of polymers, the value of k lies typically in the range of 10^{-3}–10^{-4}. However, PEI showed k value in the order of 10^{-2}. PEI is a hard amorphous polymer and a larger fraction of volume of material is removed during impact. However, Eq. 1 provides only a rough estimate of the factors controlling erosive wear; because it ignores the effect of variation of the impact angle.

Effect of impact angle (α) and impact velocity (v)

The impact angle and the impact velocity are the most important impingement variables which influence the erosion behavior of materials. The impact angle in erosion is defined as the angle between the direction of particle motion and the target surface, so that normal impact corresponds to an impact angle of 90°. The steady-state erosion rates are plotted against impact angle (α) at different impact velocities that is shown in Fig. 4. It is observed that all the polymers showed peak erosion rate (E_{max}) at 30° impact angle and minimum erosion rate (E_{min}) at normal incidence (90°). Generally, it has been recognized that peak erosion exists at low impact angles (15–30°) for ductile materials and at a high impact angle (90°) for brittle materials. The erosion behavior of polymeric materials strongly depends up on the nature of the resin. Thermosetting polymers, such as epoxy and phenolic resins, show brittle erosion where as the erosion response of thermoplastics is of ductile type [37]. It is also observed from Fig. 4 that the steady-state erosion rate at 90° impact angle is approximately about 1/2 to 1/3 of the peak erosion rate. Hence, the order of materials ranking would change with any change of variable, such as impact angle.

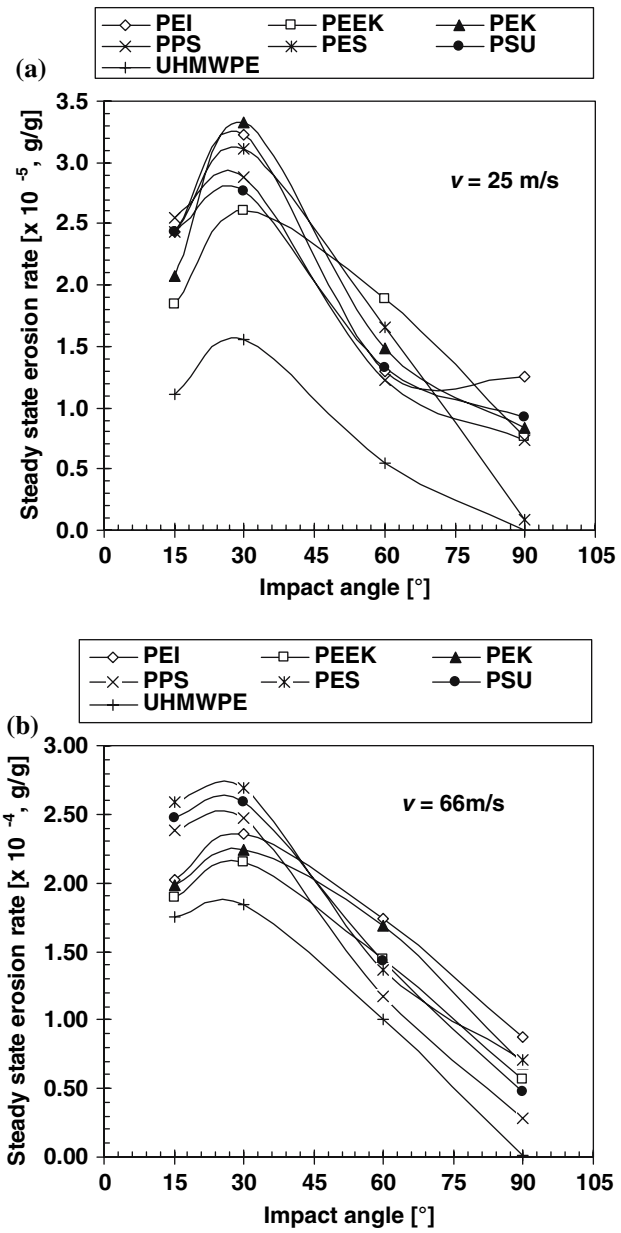

Fig. 4 Influence of impact angle on erosion rate of various polymers

Table 3 Wear coefficients of high-performance polymers at normal impact angle for different impact velocities

Polymer	Wear coefficient (k)		
	25 m/s	50 m/s	66 m/s
PEI	1.26×10^{-2}	1.19×10^{-2}	1.3×10^{-2}
PEEK	6.06×10^{-3}	6.34×10^{-3}	5.08×10^{-3}
PEK	6.88×10^{-3}	7.46×10^{-3}	8.04×10^{-3}
PPS	4.46×10^{-3}	3.06×10^{-3}	2.40×10^{-3}
PES	5.12×10^{-3}	4.92×10^{-3}	5.60×10^{-3}
PSU	4.76×10^{-3}	4.80×10^{-3}	3.74×10^{-3}

Tilly and Sage [27] have reported peak erosion rate at 30° impact angle for ductile materials, such as nylon and polypropylene matrix, whereas epoxy resin showed brittle erosion behavior with peak erosion rate at 90° impact angle. Walley et al. [14] have also reported peak erosion rate at 30° impact angle while studying erosion behavior of PE, PP, and PEEK. Wang et al. [16] have also observed ductile behavior of UHMWPE, while studying erosion behavior with coal powder and silicon dioxide as erodent. Rajesh et al. [8] also reported peak erosion rate at $\alpha = 15$–30° for a series of PAs studied at different impact

velocities. Also, similar observations were reported while studying the erosion behavior of various thermoplastic polymers by the various investigators [30–32]. However, during the erosion of polystyrene (PS), two erosion peaks near the impact angle of 20 and 50°, which have never been observed in other materials, were found by Thai et al. [10].

The steady-state erosion rates of all the selected polymers at different impact velocities and at two different impact angles are shown in the form of a histogram in Fig. 5. It can be seen from the histogram that erosion rate of all the polymers increases with increase in the impact velocity. However, UHMWPE showed least variation in the erosion rate with increase in the impact velocity at normal impact angle ($\alpha = 90°$). Also, it has shown the best erosion resistance under all impact conditions. The approximate percentage increase in the erosion rate of high-performance thermoplastic polymers with the increase in velocity from 25 to 66 m/s is listed in Table 4. The values are calculated for each material with reference to the steady-state erosion rate of UHMWPE at corresponding impact angle and velocity. UHMWPE is being considered as a high wear resistance material in abrasion or erosion wear situation and hence it is taken as the reference material. At normal impact angle, UHMWPE has shown excellent wear resistance than the other polymers because of low modulus and high rebound resilience provided the better erosion resistance. Similar kinds of observations were also made in the case of elastomers [23–25]. It is quite clear from the histogram (Fig. 5) that the performance of all the materials (except for UHMWPE at normal impact) has changed significantly with a change in impact velocity and impact angle. Hence, it is concluded that performance ranking is strongly influenced by experimental parameters.

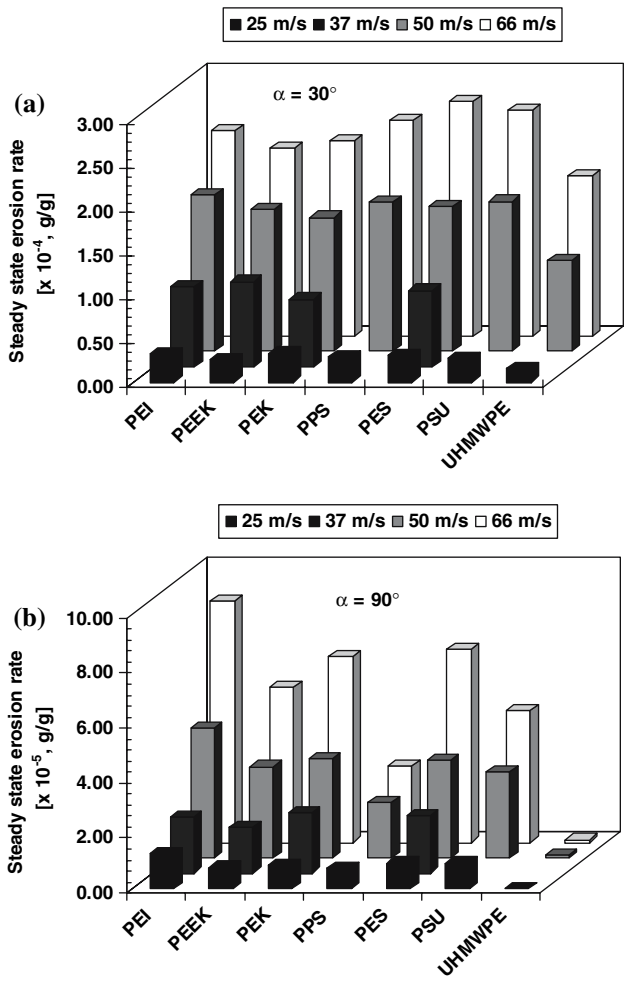

Fig. 5 Histograms showing the steady-state erosion rate of various polymers at different impact velocities

Table 4 Percentage of increase in erosion rate of high-performance polymers with respect to that of UHMWPE

Polymer	30°			90°[a]	
	25 m/s	50 m/s	66 m/s	50 m/s	66 m/s
PEI	107	72	27	4600	8670
PEEK	68	56	17	3220	5560
PEK	114	47	21	3500	6670
PPS	85	63	34	1900	2670
PES	100	60	46	3400	6900
PSU	79	65	40	3000	4700

[a] At $v = 25$ m/s, UHMWPE has not shown considerable mass loss and hence values are not reported

It is seen from Fig. 5 that the erosion rates of the polymers are significantly higher at higher impact velocities. The impinging particles have a higher kinetic energy at higher velocities which results in more wear. Figure 6 shows the variation of erosion rate as a function of particle impact velocity for various polymers at an impact angle of 90°. The dependence of erosion rate (E) on impact velocity (v) is expressed by the following equation:

$$E = Kv^n, \tag{2}$$

where n is velocity exponent and K is a constant. The values of K and n, obtained from least-square fitting to data points for the above power law at different impact angles, are summarized in Table 5. The velocity exponents are in the range of 1.4–3.0 for various polymers at different impact angles. The values of n for PPS and PSU at 90° impact angle are 1.38 and 1.71, respectively; however, the value of K is higher than that of other materials. Also, higher values of n are associated with steeper impact angles for other polymers. According to Pool et al. [34], for polymeric materials behaving in ductile manner, typically $2 < n < 3$ while for polymeric materials behaving in brittle fashion typically, $3 < n < 5$. In the present study, the values of n are in the range of 2–3 (except for PPS and PSU at $\alpha = 90°$) for all the

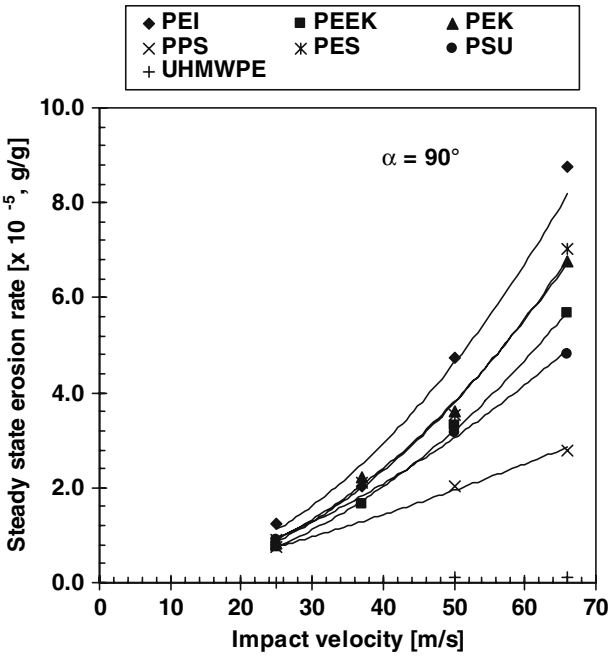

Fig. 6 Variation of steady-state erosion rate of various polymers as a function of impact velocity

materials at different impact angles. Hence, it is concluded that the high-performance polymers showed ductile erosion behavior. The influence of impact velocity on erosion rate of neat polymers has been investigated to a limited extent [10, 16, 27, 30–33]. It was reported that the value of velocity exponent (n) depends upon the nature of target material and type, shape, and size of the erodent used. Tilly and Sage [27] have reported a value of velocity exponent of 2.3, at $\alpha = 90°$, for a range of materials from metals to plastics with quartz particles as erodent (125–150 μm). For amorphous and brittle PS, Thai et al. [10] have found that the velocity exponent was 3.69 at $\alpha = 50°$. While studying the effect of impact velocity, impact angle, and the erodent type on UHMWPE, Wang et al. [16] have reported the value of n = 1.95 and 1.82 (at $\alpha = 90°$) for silica and coal powder (60–70 mesh), respectively. Miyazaki and Takeda [30] have observed the n value of 2.95 and 2.53 (at $\alpha = 30°$) for PA6 and acrylonitryl-butyldiene styrene, respectively. In the case of PEEK and TPI and their reinforced plastics, Miyazaki and Hamao [31] have reported the n value in the range of 2.0–2.5 (at $\alpha = 60°$). Hence, the present results are in agreement with those reported in the literature for ductile polymers.

Correlation of erosion data with mechanical properties of polymers

The steady-state erosion rate is dependent on polymer properties, such as hardness (H), tensile strength (S), elastic modulus (E_1), elongation to fracture (e), fracture toughness

Table 5 Parameters characterizing the velocity dependence of erosion rate of various polymers

Polymer	Impact angle (α, °)	K	n	R^2
PEI	15	2×10^{-8}	2.19	0.98
	30	4×10^{-8}	2.09	0.97
	60	3×10^{-9}	2.66	0.98
	90	1×10^{-8}	2.05	0.97
PEEK	15	1×10^{-8}	2.34	0.98
	30	3×10^{-8}	2.18	0.94
	60	2×10^{-8}	2.12	0.99
	90	1×10^{-8}	2.07	0.99
PEK	15	9×10^{-9}	2.40	0.99
	30	5×10^{-8}	2.00	0.99
	60	6×10^{-9}	2.47	0.99
	90	9×10^{-9}	2.12	0.99
PPS	15	1×10^{-8}	2.32	0.99
	30	2×10^{-8}	2.28	0.98
	60	6×10^{-9}	2.36	0.99
	90	9×10^{-8}	1.38	0.99
PES	15	1×10^{-8}	2.39	0.99
	30	3×10^{-8}	2.23	0.99
	60	2×10^{-8}	2.18	0.99
	90	1×10^{-8}	2.06	0.99
PSU	15	1×10^{-8}	2.36	0.99
	30	1×10^{-8}	2.37	0.98
	60	5×10^{-9}	2.46	0.99
	90	4×10^{-8}	1.72	0.99
UHMWPE	15	1×10^{-9}	2.91	0.99
	30	4×10^{-9}	2.59	0.99
	60	4×10^{-10}	3.00	0.99
	90	–	–	–

(K_{IC}) or fracture energy (G_{IC}), and glass transition temperature (T_g). Figure 7 indicates typical relationship obtained between steady-state erosion rates and relevant material properties for different experimental conditions. The dependence of erosion rate upon mechanical properties is complicated because the deformation caused by the erosive particles is associated with high strain rates of about 10^5–10^6 s^{-1} and the stress state is complex [14]. Hence, no single property dominates in the case of polymers.

Figure 7a shows relationship between erosion rate and hardness of various polymers. A lower hardness indicates better wear resistance and a higher hardness indicates a decrease in erosion resistance of polymers. This is due to a polymer with a lower hardness absorbs greater energy of erosive particles by elastic deformation of the target surface. Thus, a lower amount of impact energy is available for other processes, such as plastic deformation, crack

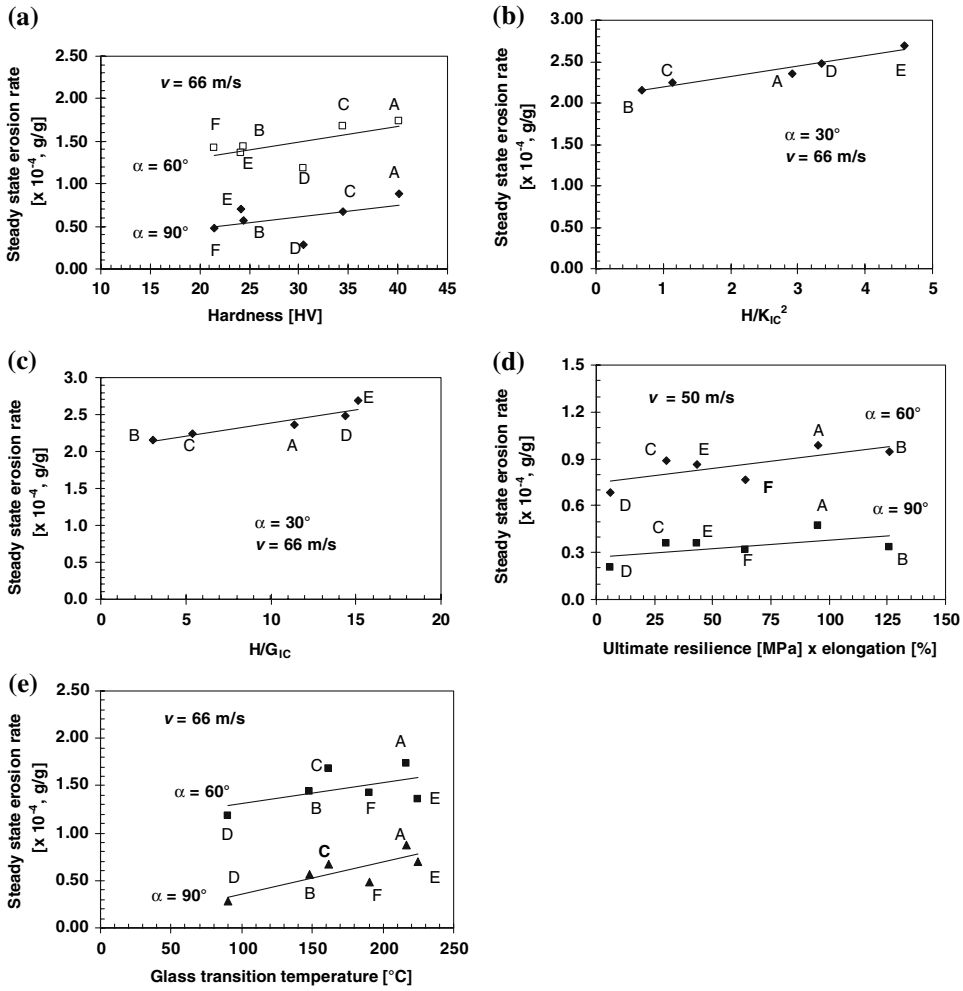

Fig. 7 Relation between steady-state erosion rates and various mechanical properties and glass transition temperature (T_g) of various polymers at different impact angles and impact velocities (A: PEI, B: PEEK, C: PEK, D: PPS, E: PES, F: PSU)

initiation, and local fracture [12]. Walley et al. [14] have also reported that for PE, PP, and PEEK, the erosion rate increased as hardness increased and ductility improved the erosion resistance.

Figure 7b, c shows relationship between erosion rates and "brittleness index" term of form $\left(H/K_{IC}^2\right)$ or (H/G_{IC}) of various polymers. It is observed that an increase in fracture toughness (K_{IC}) or fracture energy (G_{IC}) of polymers leads to an improvement in erosion resistance. Lower the "brittleness index", better the erosion resistance of polymers. Friedrich [12] has studied erosive wear of five types of polymers (PE, two types of PP, PS, and polybutadine) and reported that high fracture energy leads to an improvement in the erosion resistance of polymers. The authors have concluded that "brittleness index" is a good indicator for erosion resistance of polymeric materials. Lamy [46] has proposed the H/K_{IC} as a convenient "brittleness index" for materials subjected to surface scratching in abrasive or erosive wear processes. Wiederhorn and Hockey [47] have suggested a modified "brittleness index", $H^{0.5}/K_{IC}^2$, to describe the erosion resistance of brittle materials. Figure 7d shows the relationship between steady-state erosion rate and the product of ultimate resilience ($S^2/2E_1$) and elongation (e) of various polymers. The elastic modulus is always related to ultimate resilience [18]. As the product of ultimate resilience and elongation increases the erosion rate also increases. Kayser [21] has observed some correlations with ultimate resilience and density of material for various natural and synthetic rubbers.

Figure 7e shows correlations between erosion rate and glass transition temperature (T_g) observed for various polymers. The amorphous polymers having higher glass transition temperature erode faster than semi-crystalline polymers (Fig. 7e). The other investigators also have found correlation between erosion rate and glass transition temperature [22, 23] for various rubbers and elastomers. With reference to the influence of T_g on the erosion resistance of polymers, the following trends have been observed [2, 12].

(i) Erosion is higher for polymers with glass transition temperature above room temperature (RT) relative to those with a T_g below RT.
(ii) For T_g below RT, the wear rate decreases the grater the difference between the experimental temperature and T_g is.

From the above discussion it is clear that erosion resistance of polymers is not controlled by a single material property and also depends on experimental parameters.

Microscopic analysis of eroded surfaces

In order to identify the mode of material removal, the morphologies of eroded surfaces are observed under scanning electron microscope. The scanning electron micrographs of the eroded surfaces of the various thermoplastic polymers at impact velocity of 66 m/s are shown in Figs. 8–13. The wear mechanisms of target surface are strongly influenced by the impact angle and the impact velocity. The change in impact angle from oblique to normal changes the topography of the damaged surface very significantly.

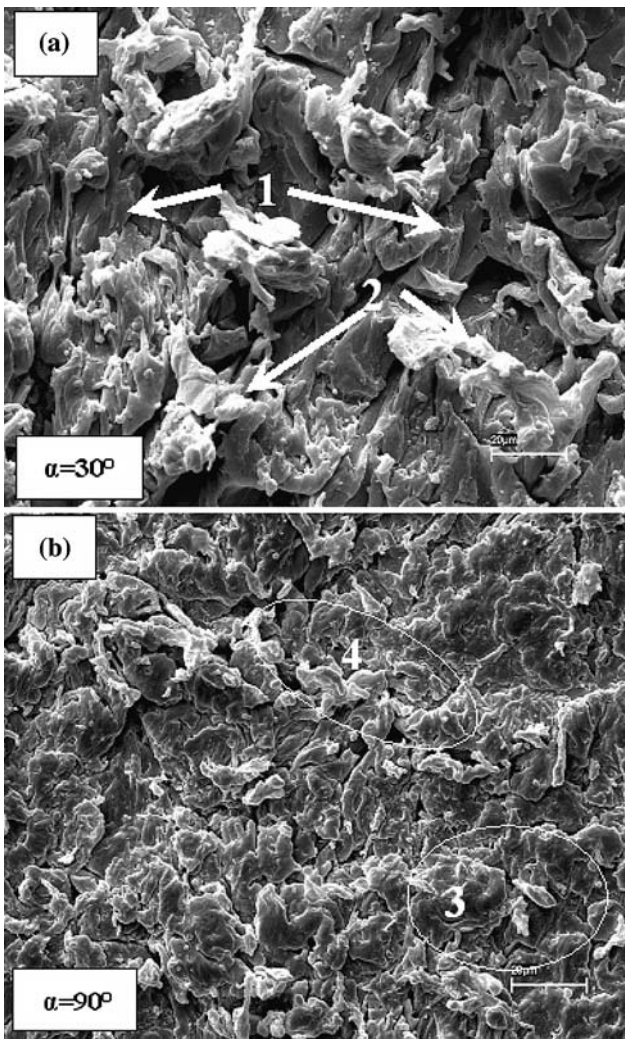

Fig. 8 Scanning electron micrographs of UHMWPE surfaces eroded at an impact velocity of 66 m/s

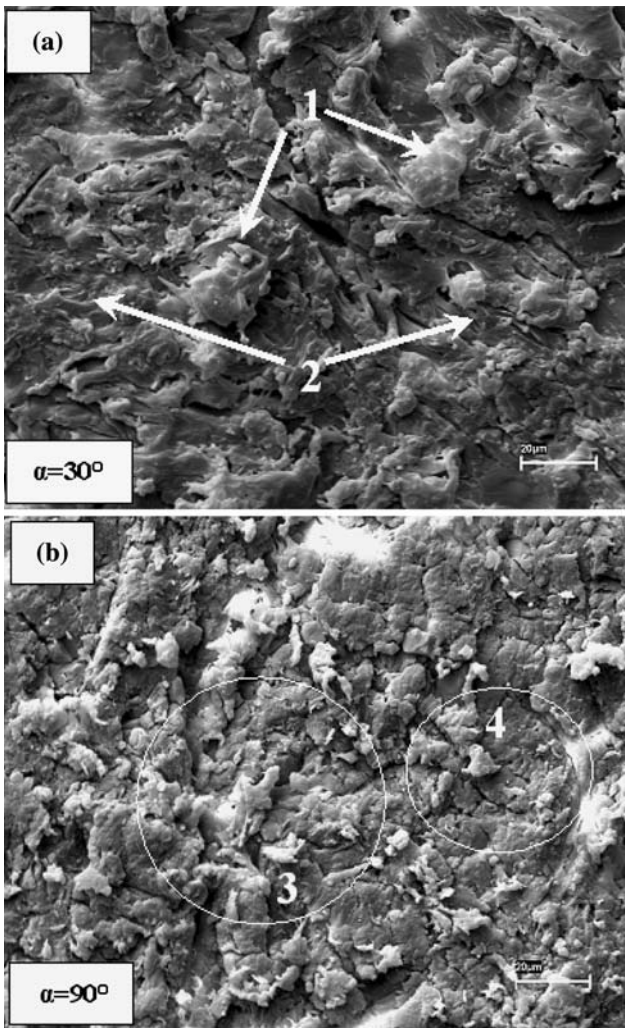

Fig. 9 Scanning electron micrographs of PEEK surfaces eroded at an impact velocity of 66 m/s

The worn surfaces of UHMWPE are shown in Fig. 8. At 30° impact angle UHMWPE is eroded by microploughing, microcutting (marked as 1), and an extensive deformation. The wear debris appears as fibrils cut from the surface which is adhered to the surface of the matrix (marked as 2). The shear lips in the form of extruded material and general ductility are evident in the micrograph. At normal impact, a network of fine cracks (marked as 3) has developed (Fig. 8b). The repeated intersection of fine cracks is also seen in the micrograph. The wear debris is still adhered to the surface (marked as 4). According to Arnold and Hutchings [24], the strain produced by a single impact is insufficient to cause the material removal. Accordingly

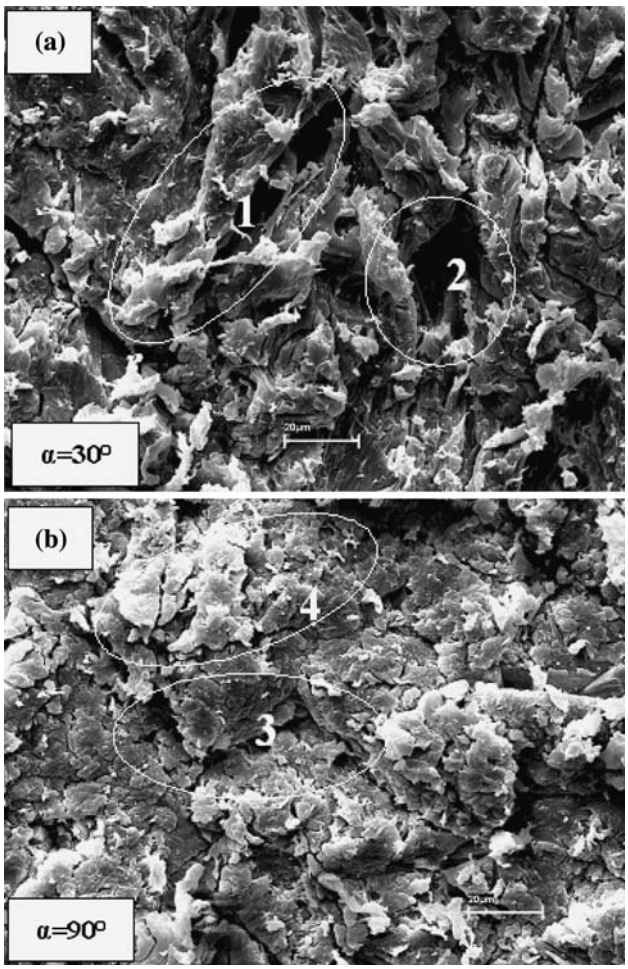

Fig. 10 Scanning electron micrographs of PEK surfaces eroded at an impact velocity of 66 m/s

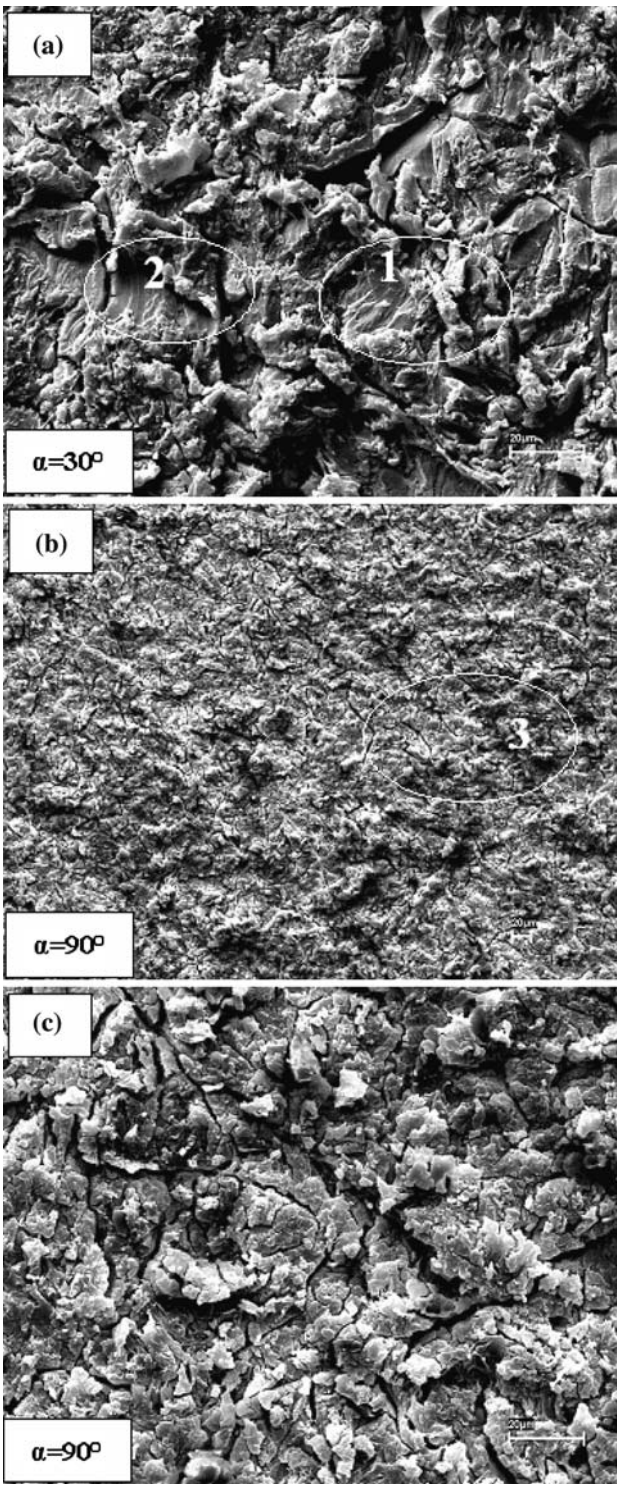

Fig. 11 Scanning electron micrographs of PEI surfaces eroded at an impact velocity of 66 m/s

successive impacts are necessary to raise the strain level linked to the material removal. This mechanism would explain the greater erosion resistance observed at normal impact for resilient materials, such as UHMWPE and elastomers. UHMWPE has shown the best erosion resistance at all impact angles and it needs a more impact time to reach steady state. Therefore, existence of the incubation period indicates a better erosion resistance. During the incubation period substantial amount of impact energy is dissipated in roughening the target surface. Similar kinds of observations were also made by Barkoula et al. [9], while studying erosion behavior of epoxy resin modified by hygrothermally decomposed PU.

Micrographs of eroded surfaces of PEEK are shown in Fig. 9. PEEK is a semi-crystalline, ductile, and tough polymer. It has shown the best wear resistance after UHMWPE at impact velocity of 66 m/s and impact angle of 30°. The wear mechanism is dominated by extensive plastic deformation (marked as 1) and microcutting (marked as 2) and removal of small flakes like debris at oblique impact angles (Fig. 9a). During normal impact, wear mechanism is dominated by plastic deformation (marked as 3) and propagation of multiple cracks (marked as 4) in all directions (Fig. 9b). The micrograph also indicated small impact crater, it is expected that several

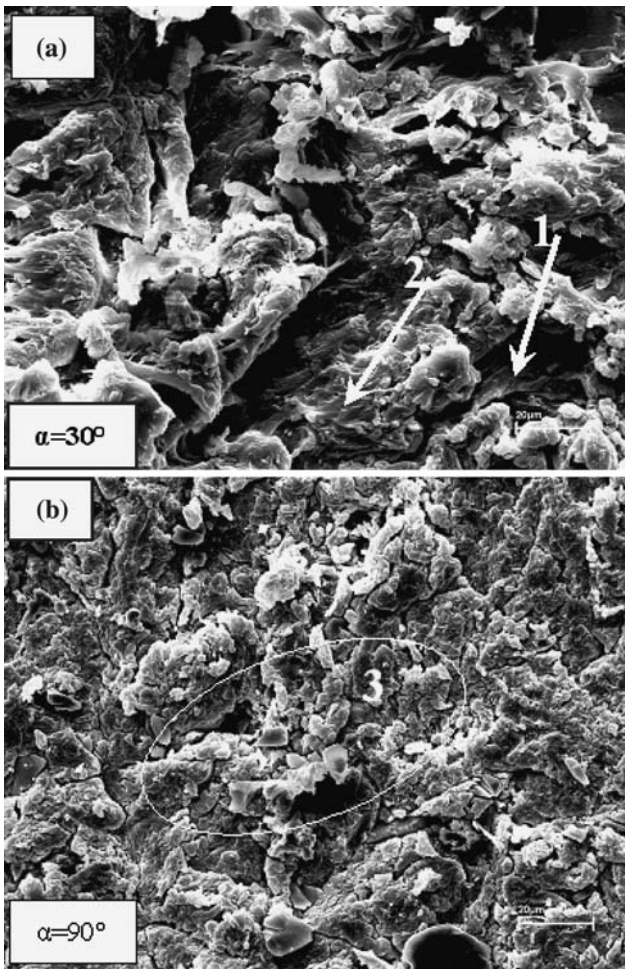

Fig. 12 Scanning electron micrographs of PPS surfaces eroded at an impact velocity of 66 m/s

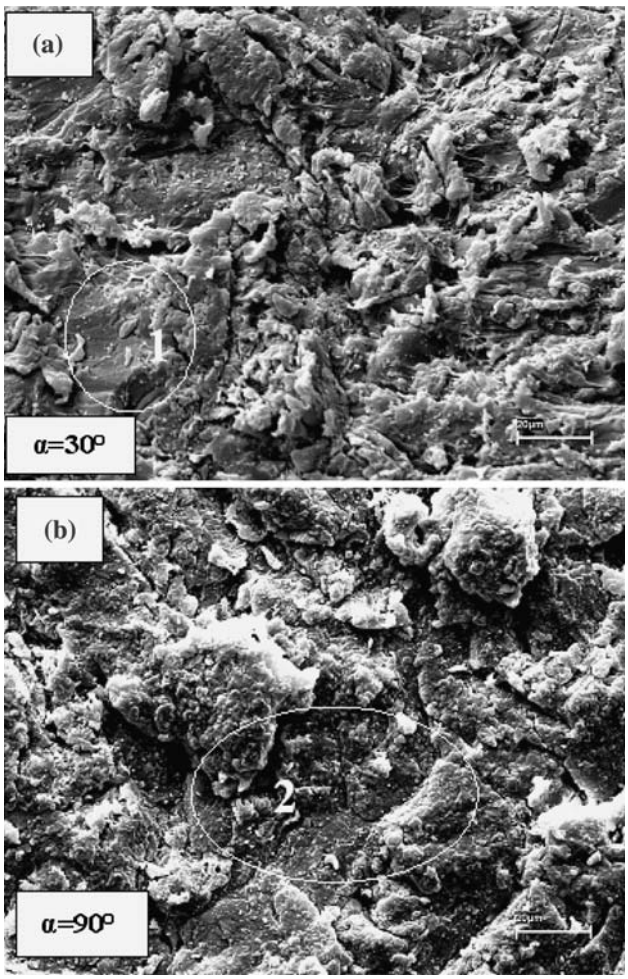

Fig. 13 Scanning electron micrographs of PES surfaces eroded at an impact velocity of 66 m/s

cumulative impacts are required for material removal in ductile polymer.

The worn surfaces of PEK under different impact conditions are shown in Fig. 10. The erosion mechanism at oblique impact angle is fully dominated by ductile tearing (Fig. 10a). Micrograph clearly shows a large degree of fibrillation of matrix before they break (marked as 1). The eroded surface also showed localized pit formation (marked as 2). At normal impact (Fig. 10b), dense deep microcracks are present in the surface (marked as 3). These dense networks are caused by residual tensile stresses in the surface after repeatedly being impacted. The thin platelets are removed by repeated impacts. These eventually become detached and would be expected to form plate like debris (marked as 4).

Micrographs of eroded surfaces of PEI are shown in Fig. 11. Typical characteristic features of abrasion marks and small groves (marked as 1) due to erosion are seen at oblique impact angle (Fig. 11a). It is also evident from the micrograph that microcutting (marked as 2) is the dominating mechanism of material removal. PEI is an amorphous ductile polymer. However, the failure mode does not reflect any ductility instead a brittle failure in the micrograph. During normal impact, the propagation of cracks along transverse as well as longitudinal directions (marked as 3) can be seen in the micrograph of lower magnification (Fig. 11b). At higher magnification the network of these cracks can be clearly seen (Fig. 11c). This cracking is aggravated due to multiple impacts probably by fatigue mechanism.

Micrographs of eroded surfaces of PPS are shown in Fig. 12. Typically very wide grooves due to microcutting and microploughing (marked as 1 and 2) can be seen in the micrograph at oblique impact angle (Fig. 12a). At normal impact angle, visual inspection indicated blackening of eroded surface. This is due to low thermal conductivity and low glass transition temperature (T_g) of PPS. Also high temperatures known to occur in solid-particle erosion, softening of the matrix due to repeated impacts led to surface degradation of the target material [5, 27, 34].

Micrograph (Fig. 12b) indicated typical network of microcracks (marked as 3) at normal impact angle.

Micrographs of the eroded surfaces of PES are shown in Fig. 13. At an oblique impact angle, matrix removal took place by typical microchipping (marked as 1) and wear debris removed like thin platelets (Fig. 13a). At normal impact angle, the removal of material is due to intersection of cracks that can be seen from the micrograph (Fig. 13b). Also formation of small crater (marked as 2) can be seen in the micrograph. It is observed from the micrographs (Fig. 13a, b) that the wear mechanism is dominated by brittle failure.

Conclusions

1. The selected polymers in the present study exhibited maximum erosion rate at 30° impact angle and minimum at 90° impact angle indicating ductile behavior.
2. An incubation behavior was found for PEEK, PPS, and UHMWPE at normal impact angle. The incubation period decreases with an increase in particle impact velocity. No incubation was observed in the case of PEI, PEK, PES, and PSU.
3. Ranking of the polymers changes with the experimental conditions like impact angle and impact velocity. The erosion rate of polymers increased by one order of magnitude when impact velocity varied from 25 to 66 m/s.
4. PEEK has shown a better erosion resistance than the other polymers at oblique impact angles (15 and 30°) for two different impact velocities (25 and 66 m/s). Whereas at higher impact angles (60 and 90°), PPS has shown a better erosion resistance due to softening of matrix (low glass transition temperature $\approx$ 90° C) and embedment of erodent particles.
5. Mechanical properties, such as hardness, fracture toughness, tensile strength, and ultimate elongation play a prominent role in controlling the erosive wear of polymers. The glass transition temperature (T_g) is also seems to have an important effect on solid-particle erosion of polymers.
6. SEM studies reveal that microcutting, microchipping, microploughing, ductile tearing, and plastic deformation are dominating wear mechanisms at oblique impacts whereas under normal impact, material removal takes place by microcracking and plastic deformation.

References

1. Johnston NJ, Towell TW, Hergenrother PM (1991) Thermoplastic composite materials. Elsevier Science Publishers, BV, p 27
2. Barkoula N-M, Karger-Kocsis J (2002) J Mater Sci 37:3807
3. Hutchings IM (2002) Tribology: friction and wear of engineering materials. Butterworth-Heinemann, Oxford, p 174
4. Arjula S, Harsha AP (2006) Polym Test 26:188
5. Tilly GP (1969) Wear 14:63
6. Smeltzer CE, Gulden ME, Campton WA (1970) J Basic Eng 92:639
7. Ratner SB, Styller EE (1981) Wear 73:213
8. Rajesh JJ, Bijwe J, Tewari US, Venkataraman B (2001) Wear 249:702
9. Barkoula NM, Gremmels J, Karger-Kocsis J (2001) Wear 247:100
10. Thai CM, Tsuda K, Hojo H (1981) J Test Eval 9:359
11. Walley SM, Field JE Yennadhiou P (1984) Wear 100:263
12. Friedrich K (1986) J Mater Sci 21:3317
13. Walley SM, Field JE (1987) Phil Trans R Soc Lond A 321:277
14. Walley SM, Field JE, Scullion IM, Heukensfeldt Jansen FPM, Bell D (1984) In: Field JE, Dear JP (eds) Proceedings of seventh international conference on erosion by liquid and solid impact. Cavendish Laboratory, Cambridge, UK, p 58
15. Walley SM, Field JE, Greengrass M (1987) Wear 114:59
16. Wang YQ, Huang LP, Liu WL, Li J (1998) Wear 218:128
17. Rao PV, Buckley DH (1984) ASLE Trans 27:373
18. Rao PV, Buckley DH (1986) ASLE Trans 29:283
19. Böhm H, Betz S, Ball A (1990) Tribol Int 23:399
20. Brandstädter A, Goretta KC, Routbort JL, Groppi DP, Karasek KR (1991) Wear 147:155
21. Kayser W (1967) In: Fyall AA, King RB (eds) Proceedings of 2nd Meersburg conference on rain erosion and allied phenomena. Royal Aircraft Establishment, Farnborough, UK, p 427
22. Marei AI, Izvozchikov PV (1967) Abrasion of rubber. MacLaren, London, p 274
23. Hutchings IM, Deuchar DWT, Muhr AH (1987) J Mater Sci 22:4071
24. Arnold JC, Hutchings IM (1989) J Mater Sci 24:833
25. Li J, Hutchings IM (1990) Wear 135:293
26. Besztercey G, Karger-Kocsis J, Szaplonczay P (1999) Polym Bull 42:717
27. Tilly GP, Sage W (1970) Wear 16:447
28. Williams JH Jr, Lau EK (1974) Wear 29:219
29. Häger A, Friedrich K, Dzenis YA, Paipetis SA (1995) In: Street K, Whistler BC (eds) Proceedings of ICCM-10, Canada 1995. Woodhead Publishing Ltd, Cambridge, p 155
30. Miyazaki N, Takeda N (1993) J Compos Mater 27:21
31. Miyazaki N, Hamao T (1994) J Compos Mater 28:871
32. Harsha AP, Tewari US, Venkataraman B (2003) Wear 254:693
33. Harsha AP, Thakre AA (2007) Wear 262:807
34. Pool KV, Dharan CKH, Finnie I (1986) Wear 107:1
35. Zahavi J, Schimitt GF Jr (1981) Wear 71:179
36. Mathias PJ, Wu W, Goretta KC, Routbort JL, Groppi DP, Karasek KR (1989) Wear 135:161
37. Roy M, Vishwanathan B, Sundararajan G (1994) Wear 171:149
38. Miyazaki N, Funakura S (1998) J Compos Mater 32:1295
39. Barkoula N-M, Karger-Kocsis J (2002) Wear 252:80
40. Tewari US, Harsha AP, Häger AM, Friedrich K (2002) Wear 252:992
41. Tewari US, Harsha AP, Häger AM, Friedrich K (2003) Compos Sci Technol 63:549
42. Moss E, Karger-Kocsis J (1999) Adv Compos Lett 8:59
43. Rattan R, Bijwe J (2006) Wear 262:568
44. Bull SJ (1997) Mater Sci Forum 246:105
45. Ruff AW, Ives LK (1975) Wear 35:195
46. Lamy B (1984) Tribol Int 17:35
47. Wiederhorn SM, Hockey BJ (1983) J Mater Sci 18:766